DOI 10.1002/pmic.200500243 *Proteomics* 2006, *6,* 1460–1470

RESEARCH ARTICLE

Proteomic and SAGE profiling of murine melanoma progression indicates the reduction of proteins responsible for ROS degradation

Gustavo A. de Souza[1, 2], Lyris M. F. Godoy[1, 2], Veronica R. Teixeira[3], Andreia H. Otake[3], Adão Sabino[4], José C. Rosa[1, 2], Anemari R. Dinarte[1, 5], Daniel G. Pinheiro[1, 5], Wilson A. Silva, Jr.[1, 5], Marcos N. Eberlin[4], Roger Chammas[1, 3] and Lewis J. Greene[1, 2]*

[1] Centro de Terapia Celular, Centro Regional de Hemoterapia de Ribeirão Preto, Centro de Pesquisa, Inovação e Difusão (CEPID) – FAPESP, Brasil
[2] Centro de Quimica de Proteinas, Departamento de Biologia Celular, Molecular e Bioagentes Patogênicos, Faculdade de Medicina de Ribeirão Preto, Universidade de São Paulo, Ribeirão Preto, SP, Brasil
[3] Laboratorio de Oncologia Experimental LIM-24, Faculdade de Medicina, Universidade de São Paulo, São Paulo, SP, Brasil
[4] Laboratorio Thomson de Espectrometria de Massa, Instituto de Química, Universidade de Campinas, Campinas, SP, Brasil
[5] Laboratorio de Genética Molecular e BioInformática, Centro Regional de Hemoterapia de Ribeirão Preto, Ribeirão Preto, SP, Brasil

Using 2-DE of total cell protein extracts, we compared soluble proteins from murine melanoma lines Tm1 and Tm5 with proteins from the nontumoral cell melan-a from which they were derived. Seventy-one of the 452 spots (average) detected with CBB were differentially accumulated, *i.e.*, increased or decreased twofold. Forty-four spots were identified by PMF/MALDI-TOF, 15 with increased and 29 with decreased protein levels. SAGE showed that 17/34 (50%) of the differentially accumulated proteins, p*I* range 4–7, presented similar differences at the mRNA level. Major reductions in protein were observed in tumor cells of proteins that degrade reactive oxygen species (ROS). Decreases of $\geq$ twofold in GST, superoxide dismutase, aldehyde dehydrogenase, thioredoxin, peroxiredoxin 2, and peroxiredoxin 6 protein were observed. SAGE indicated the reduction of other proteins involved in ROS degradation. As expected, the accumulation of exogenous peroxides was significantly higher in the tumor cells while the levels of glutathionylation were two times lower in the tumor cells compared to melan-a. The differential accumulation of proteins involved in oncogene/tumor suppressor pathways was observed. Melanoma cells can favor survival pathways activated by ROS by inhibiting p53 pathways and activation of Ras and c-myc pathways.

Received: April 15, 2005
Revised: August 16, 2005
Accepted: August 22, 2005

Keywords:
Mass spectrometry / Melanoma progression / Proteome / Reactive oxygen species / SAGE

Correspondence: Professor Lewis J. Greene, Centro de Quimica de Proteinas, Fundacão Hemocentro de Ribeirão Preto, R.Ten. Catão Roxo 2501, 14051–140 Ribeirão Preto, SP, Brasil
E-mail: ljgreene@fmrp.usp.br
Fax: +55-16-2101-9366

Abbreviations: DHE, dihydroethidium; **ROS**, reactive oxygen species

1 Introduction

Melanoma progression is a multistep process which involves an unidentified sequence of genetic events resulting in aberrant gene expression [1]. Functional consequences are com-

* Additional corresponding author: Professor Roger Chammas, **E-mail**: rchammas@lim24.fm.usp.br

plex and affect several biological processes such as control of the cell cycle [2], apoptosis [3], enzymatic hydrolysis of the extracellular matrix [4], local immunosuppression and mechanisms of immunological escape [5, 6], angiogenesis [7], and cell migration [8]. Melanomas in the early stages of development are curable, but the prognosis of individuals with metastatic melanoma is poor, with a 5-year survival rate of approximately 12% [9, 10]. Consequently, the identification of the molecular events involved in the progression of metastatic melanomas is of clinical importance.

The *in vitro* characterization of melanoma cells has demonstrated several differences from normal melanocytes. The main differences are in groups of proteins related to the ability to survive in different environments, facilitating migration and metastasis. It has been shown that the repertoire of proteins involved in cell-cell and cell-extracellular matrix adhesion changes during melanoma progression, as normal cells advance toward a more invasive phenotype. Although not detected in the present study, it has recently been shown by others that melanocytes express E-cadherin, a protein involved in cell-cell adhesion of epithelial tissues, while melanoma cells express N-cadherin, a protein characteristic of connective tissue. This change in protein expression results in the escape of melanoma cells from the negative control of keratinocytes, while gaining new affinities for fibroblasts, thus facilitating invasion [11, 12].

Recently proteomics, cDNA microarrays, and SAGE have been used to identify proteins associated with melanoma progression [13–18]. Several proteins such as nucleophosmin [17], secreted acidic cysteine-rich glycoprotein (SPARC) [16], macrophage migration inhibitory factor (MIF) [16], and RhoC [13] were identified in various melanoma cell lines by these methods. However, the complex etiology of this disease makes the characterization of molecular events difficult and, even more importantly, the cells used to compare stages of melanoma progression were not derived from the same line.

In the present study, we used a tumor progression model consisting of melan-a [19] and two tumoral cell lines, Tm1 and Tm5, having a vertical growth phase phenotype and derived from melan-a, after selection by anchorage-independent growth [20]. The objective of the research was to compare the normal melanocyte cell line with the two melanoma cell lines derived from it using proteomic and SAGE analysis to identify critical molecules and/or pathways involved in melanoma progression and, when possible, to extend these data by carrying out parallel functional studies. Major changes of abundance were observed for enzymes involved in the degradation of reactive oxygen species (ROS). SAGE data were in agreement with about 50% of the results obtained by proteomic analysis and, in addition, SAGE revealed a general down-regulation of other proteins involved in ROS degradation in the tumor lines. The biological consequences of the modifications observed in the proteomic analysis were tested in separate experiments by comparing the level of total protein glutathionylation and the rate of clearance of exogenously added H_2O_2 in melan-a and the tumor cells. As expected from the proteome and SAGE data, the accumulation of peroxides was significantly higher in the tumor cells than in the normal cell line from which they were derived (Fig. 3) while the levels of glutathionylation were two times lower in the tumor cells to melan-a (Fig. 4).

2 Methods

2.1 Cell culture

Cells were grown in bovine fetal serum-free OPTI-MEM medium, (Invitrogen-Gibco), pH 6.9, containing 200 nM phorbol ester acetate (Invitrogen-Gibco) in a humid atmosphere with 5% CO_2 at 37°C. Cells in the logarithmic phase were washed with Hanks solution at 4°C, collected with a cell scraper, counted, and then lysed as described in Section 2.2.

2.2 Lysis and protein solubilization

Cells (1×10^7) were resuspended in 500 μL of protein extraction buffer (8 M urea, 2% CHAPS w/v, 1 mM PMSF). They were submitted to three cycles of sonication at 4°C and then centrifuged at 18 500*g* for 30 min at 4°C (Model 5804, Eppendorf). The supernatant was collected and total protein was measured by the Bradford method [21] using BSA as standard.

2.3 2-DE

IEF was performed with Immobiline pH 4–7 gradient (IPG) strips, 18 cm long (GE Healthcare-Amersham) in an IPGPhor electrophoretic system (GE Healthcare). The total protein extract (1 mg) was applied to the IPG strip during rehydration, as described by Rabilloud *et al.* [22]. Rehydration was carried out with 8 M urea, 2% CHAPS w/v, 65 mM DTT, 0.5% IPG buffer v/v, and traces of bromophenol, added to the sample to a final volume of 400 μL. Electrophoresis was carried out overnight using 50 μA/strip and 150 V for 1 h, 500 V for 1 h, 1000 V for 1 h, and 8000 V until 70 000 Vh were accumulated.

After IEF, strips were reduced with 65 mM DTT for 15 min in equilibrium buffer (50 mM Tris-HCl, 6 M urea, 2% SDS w/v, 30% glycerol v/v, and traces of bromophenol, pH 8.0), followed by alkylation for 15 min by the addition of 100 mM iodoacetamide in equilibrium buffer. All reagents were of Plus One quality (GE Healthcare). These selective conditions gave the largest number of separated proteins.

SDS-PAGE was carried out in an Ettan Dalt-Six electrophoretic system (GE Healthcare), using homogeneous 12.5% polyacrylamide gels of 1.5 mm thickness [23]. The IEF strip was placed on top of the gel, fixed with 0.5% agarose w/v and submitted to electrophoresis (20 mA/gel, 300 V, 6 W) at 10°C until the bromophenol left the gel (about 16 h). Proteins were detected in the 2-DE gel with colloidal CBB

G-250 staining (Serva Electrophoresis GmbH, Heidelberg, Germany) [24]. Other reagents used during staining were products of Merck, analytical grade.

2.4 2-D gel scanning and analysis

After staining, gels were scanned using the ImageScanner data acquisition system (GE Healthcare). Spot detection, mapping, spot volume determination, and comparisons between gels were performed using ImageMaster-2D software, version 4.01 (GE Healthcare). The 2-D maps obtained from melan-a, Tm1, and Tm5 contained an average of 452 spots.

The comparisons between 2-D maps of melan-a, Tm1, and Tm5 cells were made only on the basis of spots present in all three replicate gels of each cell type. At least 90% of the spots with high staining intensity (>400) were detected at the same location in all three replicates for each cell type. Analysis of 20 spots present in each of the three replicates prepared from a single lysate of each cell type indicated that the SD of protein spot intensity was less than 40%. On this basis, we defined protein accumulation or reduction as an increase or decrease of more than twofold (100%), *i.e.*, $\geq$2 SD, when the same spots in different cell lines were compared. The differences observed amongst cell types paralleled the reduced peroxide metabolism.

The p*I*, molecular weight (MW), and normalized volume (proportional to protein content) of the spots corresponding to differentially accumulated proteins were calculated for each type of cell from data obtained for nine gels.

2.5 Sample preparation for MS

Spots corresponding to differentially accumulated proteins were submitted to tryptic digestion *in situ* as described by Williams and Stone [25]. After excision from the gel, spots were washed with 200 μL of 0.1 M NH_4HCO_3, pH 8.0, containing 50% ACN, until elution of SDS and the CBB stain. Spots were then incubated with 100% ACN for 20 min and dried in a vacuum concentrator (SpeedVac AS290, Savant). Samples were rehydrated with 5 μL of 0.1 M NH_4HCO_3 containing 0.4 μg trypsin (MS grade, Promega). After rehydration, 50 μL of buffer was added to the sample and digestion was performed for 24 h at 37°C. The reaction was stopped with 5% TFA. Peptides were eluted from the gel three times with 100 μL of 50% ACN containing 2.5% TFA, and the supernatants were combined, concentrated to 5 μL and cleaned with C18 resin (Poros) in a pipette tip.

2.6 MS

Peptide mass fingerprint analysis was done with a MALDI-TOF model Maldi LR (Micromass, Manchester, UK). Peptides were diluted 1:5 in the organic matrix (1% CHCA, 50% ACN, 0.2% TFA), crystallized on the MALDI plates, and submitted to ionization. Calibration was done using a mixture of: angiotensin I (1297.51 Da), ACTH 1–17 (2094.35 Da), ACTH 18–39 (2466.74 Da), ACTH 7–38 (3660.22 Da), and bovine insulin (5734.60 Da).

2.7 Databank searches

Ions identified by MS were analyzed with the MS-Fit tool (Protein Prospector–http://prospector.ucsf.edu) using the Swiss-Prot databank for human-mouse proteins (except for spots 15 and 24, which were identified only using the NCBInr databank). The parameters used for the search were 0.2 Da for permitted mass error and one missed cleavage site for trypsin hydrolysis specificity. Proteins were identified on the basis of a minimum sequence coverage of more than 15%. Functional protein classification was based on level 5 of the Gene Ontology classification, available at http://source.stanford.edu.

2.8 SAGE

Total RNA was prepared from 4×10^7 melan-a, Tm1, or Tm5 cells obtained from a fresh culture using TRIzol® LS Reagent (Invitrogen) and treated with RQ1 RNase-Free Dnase (Promega). Thirty milligram of total RNA was then used for the SAGE procedure, which was carried out with the I-SAGE kit (Invitrogen) [26]. Tag frequency tables were constructed from sequence data by the SAGE analysis software, with the minimum tag count set at 1 and the maximum ditag length set at 28 bp, and the parameters were set as default. The annotation was based on the SAGEmap database (http://www.ncbi.nlm.nih.gov/SAGE/). Statistical analysis was carried out with the H2G software (hyper- and hypo-expressed Genes) for the comparison of two SAGE libraries. The H2G software was also used to perform the normalization of compared libraries, using as reference the library with the highest number of annotations. Most representative differentially expressed genes were selected on the basis of normalized tag frequency higher then 30.

2.9 H_2O_2 degradation

Melan-a, Tm1, and Tm5 cells were cultured in the presence of 100 μM H_2O_2 for varying periods of time (0.5–3 h). Intracellular peroxide content was then measured after 30-min incubation and then hourly up to 3 h with 1 μM dihydroethidium (DHE) at 37°C using a flow cytometer (FACScalibur). Peroxide-oxidized DHE binds DNA emitting a bright red fluorescence, read at FL-2 PMT, when cells are excited with Ar laser light (488 nm) [27].

2.10 Protein glutathionylation

To determine the overall level of glutathione attached to cell proteins, 60 μg of an extract of total protein from each cell line was submitted to nonreducing 12.5% SDS-PAGE, followed by protein transfer to an NC membrane using a

MiniVE electrophoretic system (GE Healthcare). A mouse mAb against glutathione (Chemicon) was used at 1:500 dilution, and visualized with a donkey secondary antibody to mouse immunoglobulin (GE Healthcare) at 1:2500, using a chemoluminescence imaging kit (GE Healthcare) followed by exposure to X-ray film (Kodak). The film was scanned with an ImageMaster scanner (GE Healthcare) and band intensities were measured with ImageMaster 2D software.

3 Results

3.1 Analysis of differentially accumulated proteins

A representative 2-DE gel of the total protein extract of melan-a cells is shown in Fig. 1A. The tumor forms of melan-a, Tm1, and Tm5 had very similar, almost identical, spot profiles on 2-DE, which facilitated comparison and per-

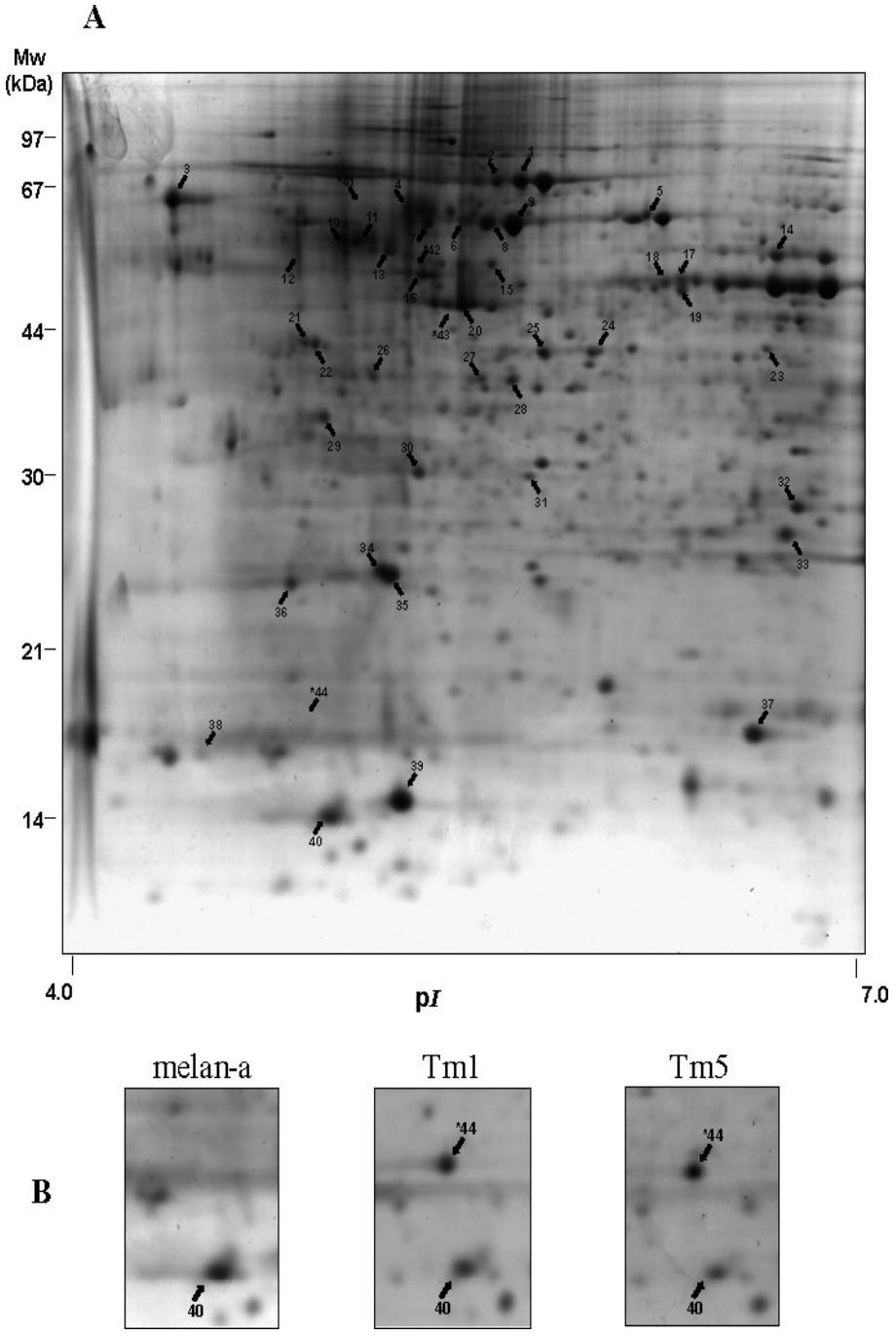

Figure 1. Representative 2-DE map of melan-a cells. Panel A: 1 mg of a total protein extract of melan-a cells was submitted to IEF using 4–7 p*I* strips, followed by SDS-PAGE in 12.5% polyacrylamide gel. Numbered spots indicate differentially accumulated proteins identified by MALDI-TOF MS which are listed in Table 1, column 1. Panel B: Numbers with an asterisk indicate the position of spots detected in 2-DE maps of extracts of Tm1 and Tm5 cells but not visible in melan-a gels. The mass markers were assigned on the basis of standard proteins not visible in the figure.

Table 1. Differentially accumulated proteins during melanoma progression from melan-a to Tm1 and Tm5

1. Spot	2. Identified protein	3. Sequence covered, %	4. Access number Swiss-Prot	5. Proteomics		6. SAGE		7. Mass/p/2-DE	8. Mass/p/Swiss-Prot
				Tm1/m-a	Tm5/m-a	Tm1/m-a	Tm5/m-a		
1	Stress-70 Protein (G)	21	P38647	0.31	0.23	0.23	0.2	72.261/5.58	
2		16		0.34	0.34			72.235/5.50	73.529/5.9
7		19		0.55	0.8			65.031/5.26	
3	Calreticulin	20	P14211	3.83	3.40	0.5	0.5	69.549/4.36	47.995/4.3
4		28		a)	0.34			66.914/5.23	
10	Vimentin (G)	18	P20152	a)	a)	1.0	5.19	62.345/4.98	53.688/5.1
12		45		a)	a)			61.547/4.80	
5	T-complex protein 1, epsilon subunit (N,G)	19	P80316	a)	a)	0.33	0.86	65.617/6.03	59.625/5.7
6	HSP60 (G)	17	P19226	0.9	a)	1.45	1.98	65.775/5.39	
8		26		2.00	0.84			65.278/5.47	60.956/5.9
9		37		3.35	2.56			64.932/5.56	
11	Tubulin beta chain	24	P05218	16.73	22.08	8.82	5.13	62.174/5.13	49.671/4.8
28		23		0.43	0.5			43.597/5.55	
13	ATP synthase beta chain	42	P56480	1.21	2.00	1.18	1.67	60.662/5.12	56.301/5.2
14	Aldehyde dehydrogenase	15	P47738	0.17	0.3	1.00	2.59	58.442/6.45	56.382/6.6
15	Similar to M6P receptor-binding protein (N)	21	26340270	0.81	0.45	0.23	11.67	58.509/5.48	46.886/6.0
16	Heterogeneous nuclear ribonucleoprotein F (N)	28	P52597	0.35	0.5	1.00	1.00	57.223/5.24	45.672/5.4
17	Alpha enolase (G)	29	P17182	0.45	1.00	3.61	4.63	54.975/6.15	47.141/6.4
18		26		0.5	0.63			54.858/6.09	
24	Enolase/myc-binding protein (G)	20	P17182	0.5	0.39	1.00	1.73	46.045/5.83	47.141/6.4
19	Ornithine aminotransferase (N)	29	P29758	a)	a)	4.59	6.48	53.738/6.15	48.355/6.2
20	Actin (G)	42	P02570	2.24	2.23	1.27	1.51	52.633/5.39	41.737/5.3
21	Nucleophosmin (G)	29	Q61937	4.29	1.00	7.08	4.04	47.575/4.83	32.560/4.6
22		29		4.21	2.0			47.503/4.87	
23	LIM and SH3 domain protein 1	25	Q14847	0.46	a)	0.46	0.25	45.329/6.46	29.717/6.6
25	Eukaryotic translation initiation factor 3 subunit 2 (N)	27	Q9QZD9	0.35	0.31	1.15	0.65	46.224/5.66	36.461/6.4
26	Elongation factor 1 delta	39	P57776	0.5	0.67	1.14	1.33	43.612/5.06	31.293/4.9
27	F-actin capping protein (N,G)	29	P47753	a	a)	1.09	1.08	43.515/5.45	32.940/5.3
29	Tropomyosin alpha 3 chain (G)	20	P06753	2.09	0.86	0.54	0.61	38.873/4.90	32.819/4.7
30	Ran-specific GTPase-activating protein (N,G)	35	P43487	a)	a)	0.41	0.86	34.109/5.22	23.310/5.2
31	6-phosphogluconolactonase (N,G)	21	O95336	0.39	a)	0.71	1.44	33.831/5.61	27.547/5.7
32	Peroxiredoxin 6 (N,G)	53	O08709	0.19	a)	0.69	0.54	30.060/6.56	24.874/5.7
33	GST P1	34	P19157	0.31	0.23	0.77	1.05	27.966/6.52	23.609/7.7
34	Peroxiredoxin 2 (N,G)	48	Q61171	0.3	0.36	1.00	1.00	26.358/5.09	21 779/5.2
35	Phosphatidyl ethanolamine-binding protein	56	P70296	1.11	0.4	1.00	1.30	26.040/5.12	20.831/5.2
36	Tranlationally controlled tumor protein (N,G)	31	P14701	0.26	0.28	0.12	0.09	26.355/4.78	19.462/4.8
37	Superoxide dismutase	31	P08228	0.49	0.34	4.13	8.43	16.760/6.40	15.943/6.0
38	Myosin light chain alkali (G)	41	P16475	2.02	2.11	0.38	0.86	15.906/4.47	16.930/4.6
39	Galectin-1 (G)	66	P16045	2.00	0.77	3.82	3.8	14.172/5.15	14.866/5.3
40	Thioredoxin 1	58	P10639	0.5	0.42	1.49	1.61	13.589/4.91	11.676/4.8
41	Protein Disulfide Isomerase (G)	37	P09103	b)	b)	4.22	2.20	63.434/4.97	57.144/4.8
42	26S protease regulatory subunit 6A (N)	17	P17980	b)	b)	0.42	0.52	57.153/5.37	49.204/5.1
43	Cathepsin D precursor	19	P18242	b)	b)	0.46	0.16	49.094/5.46	44.954/6.7
44	Cytochrome b5 (N)	47	P56395	b)	b)	14.08	8.07	16.793/4.90	15.241/5.0

(N) = Protein not reported to be involved in melanoma progression (see column 2).
(G) = Protein reported to be a target of glutathionylation (see column 2).
a) Protein spot not detected in either tumor cell extract (see column 5).
b) Protein spot not detected in melan-a extract (see column 5).

mitted the detection of differentially accumulated proteins, *i.e.*, more than twofold higher or lower in protein content than the corresponding spot from melan-a cells. Of the spots that were detected in the gel, 30 increased and 41 decreased when Tm1 and Tm5 were compared to melan-a. The numbers next to some of the spots indicate that the protein was identified by MALDI-TOF MS. Spots 41–44 also marked with asterisks in Fig. 1A correspond to proteins detected in Tm1 and Tm5 melanoma cells, but not in melan-a (Fig. 1B). SAGE detected transcripts of all four proteins in each of the cell lines (Table 1, column 6).

The terms "accumulation" and "reduction" have been used in this article when there was a twofold (100% increase) or decrease of protein content. "Expression" and related genomic terms are not used for proteomic data because protein degradation data are not available. Forty-four of the 71 proteins that were differentially accumulated during tumor progression were identified by MALDI-TOF MS of tryptic peptides (Table 1). The number given to each protein in Fig. 1 is the same as the number in Table 1, column 1. The data in Table 1, column 3 indicate that the sequence coverage of the MS identifications was from 15% (spot 14–aldehyde dehydrogenase 2) to 66% (spot 39–Galectin 1). Swiss-Prot access numbers are given in Table 1, column 4.

The values given in column 5 of Table 1indicate the result of the comparison of the relative amounts of differentially accumulated proteins when each tumor cell is compared to the melan-a cells. In most cases, 66/71 proteins, the extent and direction (increased or decreased) of the differentially accumulated proteins were the same for both Tm1 and Tm5 cells when compared to melan-a cells.

The multiple entries for the same protein in Table 1 indicate that more than one electrophoretic form was identified as the same protein on the basis of the peptide mass fingerprint. Proteins detected as multiple electrophoretic forms are spots 1, 2, and 7, all identified as stress-70 protein in the Swiss-Prot databank, spots 4, 10, and 12 (vimentin), spots 6, 8, and 9 (HSP60), spots 11 and 28 (Tubulin beta chain), spots 17, 18, and 24 (α-enolase) and spots 21 and 22 (nucleophosmin). Experimental and theoretical molecular masses and p*I* are given in Table 1, columns 7 and 8, respectively. Most of the molecular masses were higher by at least 10% (29/44) or lower (2/44) than the molecular masses reported by the Swiss-Prot databank. Similarly, differences of 0.1 p*I* units lower were observed for 15/44 proteins and p*I* higher for 11/44 proteins.

3.2 SAGE

SAGE experiments were carried out to complement the proteomic data. Although it is not possible to deduce quantitative protein expression profiles from mRNA analysis, SAGE provides an overview of gene expression which can be compared qualitatively to the proteomic result. The libraries yielded 32 490 nonredundant tags for melan-a, 30 130 tags for Tm1 and 22 122 tags for Tm5. In order to obtain more reliable SAGE data to better compare with the proteomic data, we listed all the differentially expressed genes ($>2\times$) with frequency $n \geq 30$ (Table 1, Supplementary Material). We were able to identify 160 differentially expressed genes in Tm1 when compared to melan-a (90 up-regulated and 70 down-regulated in the tumoral line) and 131 differentially expressed genes in Tm5 (84 up-regulated, 47 down-regulated). Of the 34 different proteins identified in the proteomic analysis as differentially accumulated, ten proteins (stress 70 protein (hspa9a), tubulin beta chain (tubb5), enolase (eno1), actin (actb), vimentin (vim), T-complex protein 1 (cct5), superoxide dismutase (sod1), galectin 1 (gals1), protein disulfide isomerase (PDI), and cytochrome b-5 (cyb5)) are also listed in the SAGE Supplementary Material. This shows that most of the proteins identified by us in the p*I* range 4–7 (24/34 proteins) would not have been identified on the basis of SAGE data, demonstrating that deductions from mRNA transcript analysis can be misleading, as also pointed out by others [28, 29].

Column 6 of Table 1 indicates the corresponding SAGE data for the proteins identified by the proteomic study. We were able to discriminate between proteins whose differences in levels observed in 2-DE resulted from differential gene expression (SAGE and proteomic data were in agreement) or presumably were the result of posttranscriptional or posttranslational control. Of the 34 proteins identified in the present study, 17 had similar decreases/increases of expression by SAGE for Tm1 and 15 for Tm5 when compared to melan-a, as observed for the 2-DE protein profile, indicating that approximately 50% of the differentially accumulated proteins identified in the 2-DE gels did not have similar differential expression of their respective mRNAs. Correlation between the ratio of protein levels (Table 1, column 5) and transcript abundance (Table 1, column 6) in the tumor cell lines as compared to the normal counterpart was low, but significant for Tm1 *versus* melan-a cells (Spearman $r = 0.3087$, $p = 0.0415$) and absent for Tm5 *versus* melan-a (Spearman $r = 0.064$, $p = 0.67$).

Since the main group of proteins identified by the proteome data participates in the degradation of ROS, we also looked for differences in mRNA expression of proteins specifically involved in ROS degradation, but not detected by the proteome study. Figure 2 shows the expression profiles of the 25 mRNAs tags of molecules involved in ROS degradation and that were differentially expressed by at least more than two-fold during tumor progression according to SAGE data. This indicates that an overall down-regulation of these molecules (19/25 mRNAs) (Fig. 2B) occurs during melan-a tumoral progression.

The main proteomic results concerning the progression of melanoma were extended in separate experiments in which H_2O_2 degradation and glutathionylation were measured in melanoma cells and in melan-a cells from which they were derived.

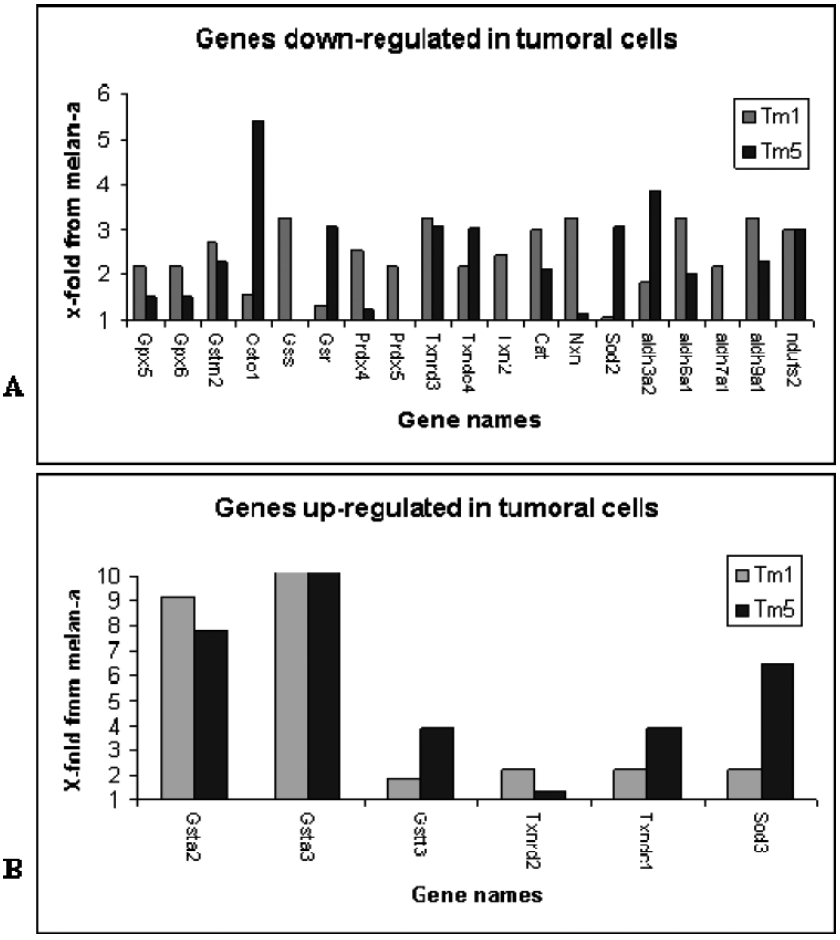

Figure 2. SAGE data for differentially expressed mRNA whose products participate in ROS degradation but were not detected by 2-DE. Most representative mRNA tag of genes that are involved in ROS degradation pathways were compared between cell lines. Only differentially expressed mRNAs (>2×) are reported. Gray bars correspond to Tm1 cells and black bars to Tm5 cells. Panel A: *Gpx5*–glutathione peroxidase 5; *Gpx6*–glutathione peroxidase 6; *Gstm2*–GST mu2; *Gsto1*–GST omega 1; *Gss*–glutathione synthetase; *Gsr*–glutathione reductase 1; *Prdx4*–peroxiredoxin 4; *Prdx5*–peroxiredoxin 5; *Txnrd3*–thioredoxin reductase 3; *Txndc4*–thioredoxin domain containing 4; *Txn2*–thioredoxin 2; *Cat*–catalase; *Nxn*–nucleoredoxin; *Sod2*–superoxide dismutase; *aldh3a2*–aldehyde dehydrogenase 3; *aldh6a1*–aldehyde dehydrogenase 6; *aldh7a1*–aldehyde dehydrogenase 7; *aldh9a1*–aldehyde dehydrogenase 9; *ndufs2*–NADH dehydrogenase Fe-S protein 2. Panel B: Genes that were up-regulated during melanoma progression. *Gsta2*–GST alpha 2; *Gsta3*–GST alpha 3; *Gstt3*–GST teta 3; *Txnrd2*–thioredoxin reductase 2; *Txndc1*–thioredoxin domain containing 1; *Sod3*–superoxide dismutase 3.

3.3 H_2O_2 degradation

Incubation of the three cell lines with the same concentration of H_2O_2 permitted us to demonstrate overall peroxide degradation measured indirectly by oxidized DHE content. DHE staining was higher in both Tm1 and Tm5 cells, peaking at 1 h of exposure to H_2O_2, as indicated in Fig. 3; melan-a cells cleared exogenous peroxides more efficiently, as indicated by the amplitude of the response at 1 h of treatment and the residual levels of peroxides after 2–3 h of exposure to H_2O_2. These data provide independent confirmation that the overall capacity of ROS degradation in Tm1 and Tm5 is decreased compared to melan-a.

3.4 Protein glutathionylation

The proteomic and SAGE data indicate that modifications of protein and gene levels of molecules involved in redox control can affect biological events in tumoral cells Tm1 and Tm5. Since the decrease of GST levels reported here is a well-characterized event in melanoma progression [30], one consequence of the reduction of the amount of the enzyme should be the decrease of overall glutathionylation of pro-

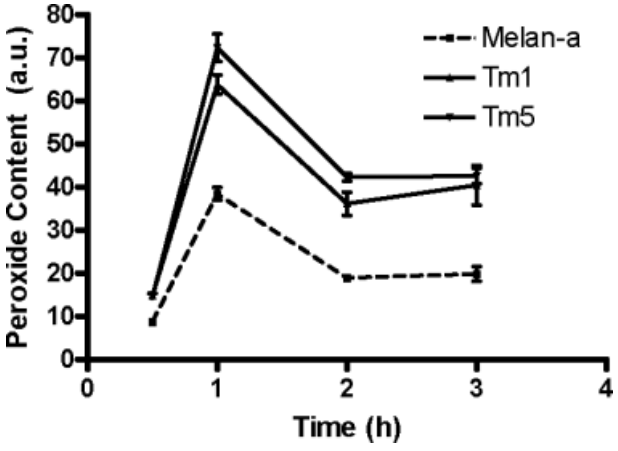

Figure 3. Tm1 and Tm5 cells accumulate higher levels of intracellular peroxides than melan-a after exposure to endogenous H_2O_2. Intracellular peroxide content was measured indirectly by flow cytometry, using the fluorochrome DHE. Data are reported as the mean fluorescence intensity ± SD of triplicate measurements. There were no differences between Tm1 and Tm5 in terms of levels of peroxide, but there was a significant decrease of peroxide concentration in Melan-a cells ($p < 0.01$, ANOVA followed by Newman–Keuls Multiple Comparison Test).

teins in the tumoral lines. We submitted total cell protein extracts to nonreducing SDS-PAGE and measured the glutathione bound to proteins with a mAb. Figure 4A shows a portion of the gel with two proteins detected by the antibody. Figure 4B shows the CBB-stained control. The volume of the bands visualized in each lane was measured and the overall level of glutathionylation was taken to be the sum of all the bands detected in each cell line. There was a statistically significant ($p < 0.01$, Student's *t*-test) reduction of glutathionylation in both Tm1 and Tm5 cell lines when compared to melan-a cells (Fig. 4C).

4 Discussion

Proteomics and SAGE have proven to be powerful tools for the identification of proteins involved in tumor progression in the present study and others [17, 31, 32]. In the present study we report the differential expression of genes and the differential accumulation of proteins in a recently described model of melanoma progression [20], which is unique in this area, because there is no other melanoma progression system in the literature in which the tumor cells were derived from the normal cell line used for comparison. We have demonstrated differential accumulation ($>2\times$ or <0.5) of 44 proteins during melanoma progression, by comparing melanoma cells Tm1 and Tm5 with melan-a cells, the cells from which the tumors were derived. Fifteen proteins were increased in quantity during tumor progression and 29 decreased. Multiple electrophoretic forms identified by MS accounted for 34% of the identified spots (16/44 spots, representing six different proteins). In addition, SAGE data complemented and extended the proteomic characterization with the measurement of the levels of transcriptional activity. Fifty percent of the proteins identified by the proteomic approach had similar (increased or decreased) mRNA expression profiles for Tm1 and Tm5 cells, suggesting that differences in expression had occurred at the gene transcription level during tumor progression. (Compare column 5 with column 6 in Table 1.)

Some of the genes identified in our SAGE analysis and/or proteome studies have been reported by others to be associated with melanoma progression. These include nucleophosmin ([17], see our Table 1), SPARC ([16], see Supplemental Material), members of the cyclin D family ([33, 34], see Supplemental Material), and Cdk2 ([35], see Supplemental material).

In addition, genes reported to be down-regulated such as galectin 3 [36] and RNA binding motif protein RBM3 [15] are also down-regulated in Tm1 and Tm5. Taken together, these data show that many of the features of our melan-a melanoma progression model are consistent with melanoma cell lines described in the literature.

Our data show the overall down-regulation and decrease of levels of proteins that participate in the ROS degradation pathways, indicating that these proteins involved in the elimination of ROS may be relevant for melanoma progression. The inability to eliminate ROS has been demonstrated by others in skin cancers, especially melanomas [37]. In general, melanomas have high levels of H_2O_2 and superoxide caused mainly by constant exposure to UV radiation [38], as a result of melanin biosynthesis [39] and down-regulation of GST, catalase, and superoxide dismutase (MnSOD), all involved in ROS elimination [30]. Our results indicate that during melanoma progression, in addition to the down-regulation of GST and MnSOD, other proteins involved in the elimination of ROS are down-regulated. These include peroxiredoxin 2 (spot 34), peroxiredoxin 6 (spot 32), thioredoxin

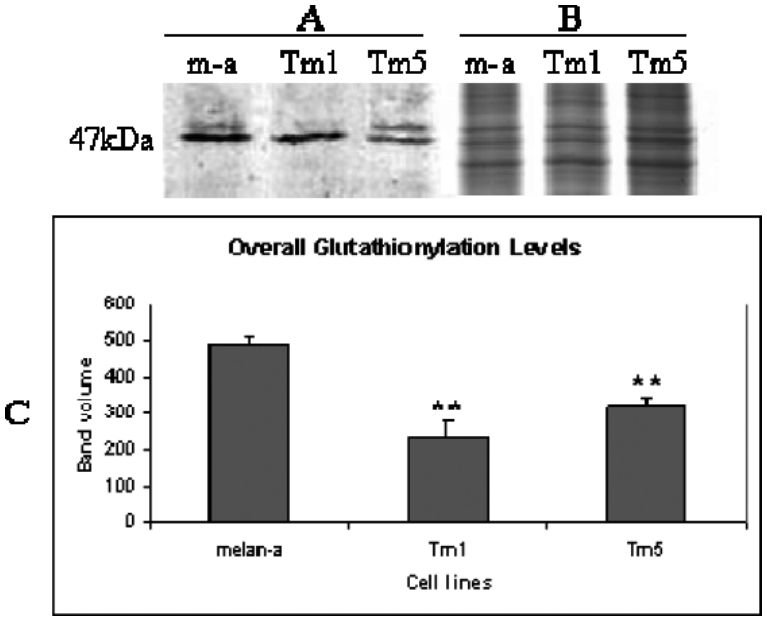

Figure 4. Protein glutathionylation is lower in melanoma cells Tm1 and Tm5 than in melanocyte melan-a cells from which they were derived. Total protein extracts of each cell line (60 μg) were submitted to nonreducing SDS-PAGE using 12.5% polyacrylamide gels. Panel A: Proteins were blotted to NC and incubated with a mouse monoclonal antiglutathione antibody. Panel B: Load control stained with colloidal CBB. Panel C: Densitometric analysis of the visible bands in the Western-blot. $*p \leq 0.01$ compared to melan-a (Student's *t*-test).

1 (spot 40), and aldehyde dehydrogenase (spot 14), indicating that the enzymes responsible for ROS degradation are reduced during tumor progression. Thus our data confirm and extend results obtained by others [30, 37] who reported that the increase of ROS in melanoma cells is the result of the decrease in the expression of GST, MnSOD, and catalase. SAGE data show that 19/25 of the mRNA tags presented decreased expression (Fig. 2). Taken together, these data demonstrate that an overall down-regulation of these genes occurs during tumor progression. By treating melan-a, Tm1, and Tm5 with H_2O_2 and then measuring the intracellular level of oxidative compounds by DHE, we demonstrated that the tumoral cells were less efficient in eliminating the hydrogen peroxide, thus demonstrating that these cells had a decreased capacity to eliminate ROS, as suggested by proteomic and SAGE data (Fig. 3)

A remarkable characteristic of the ROS activity in skin cancers is that ROS compounds such as H_2O_2 and superoxide determine the activation and expression of several proteins associated with the progression of these cancers [40]. On the other hand, ROS are considered to be toxic compounds which cause DNA damage and trigger p53-dependent apoptosis in most cell types [41, 42]. Despite this toxic activity, melanoma cells appear to activate survival pathways by ROS.

Figure 5 schematizes our proteomic data concerning ROS degradation and suggests a mechanism whereby the decrease of proteins involved in ROS elimination results in an increase of ROS levels in the tumor lines. The small arrows in Fig. 5 indicate accumulation or reduction in the amount of protein measured in tumor cell lines as compared to the levels found in the normal counterpart. The oxidative environment produced by the increase of ROS leads to several responses which include the oxidation of reduced glutathione, DNA damage, activation of NF-kB, and inhibition of the AP-1 transcription factor. DNA damage triggers both NF-kB activation and p53-dependent apoptosis. In turn, NF-kB triggers c-myc-dependent survival pathways. Accumulation of nucleophosmin (spots 21 and 22), myc-binding protein 1 (MBP-1, spot 24), galectin-1 (spot 39), and phosphatidylethanolamine-binding protein (PEBP, spot 35), all proteins involved in oncogene/tumor suppressor pathways, may explain why melanoma cells favor survival pathways in response to ROS rather than apoptotic ones.

Nucleophosmin is up-regulated in tumor cells and this protein has recently been described as a repressor of p53 activity [43] and as a potential marker for melanoma cancers [17]. Since p53 transcriptional activity can be activated by DNA damage caused by the increase of ROS levels in tumor cells, the increased expression of nucleophosmin in melanoma cells can be important to maintain cell viability and to escape apoptotic signaling. On the other hand, both tumor cells had decreased levels of myc-binding protein (MBP-1), an inhibitor of the promoting activity of c-myc oncogene [44]. In addition, the Ras oncogenic pathway can be activated by an increase in the levels of galectin 1, which acts as an amplifier of Ras signaling [45, 46], and by a decrease of PEBP, also named Raf kinase inhibitor protein (RKIP) [47, 48], whose decrease in expression is intimately associated with an increase of Ras signaling during melanoma progression [49]. Finally, the increase in PDI may act as a protective response against DNA damage, as reported for other models of oxidative-reductive stress [50].

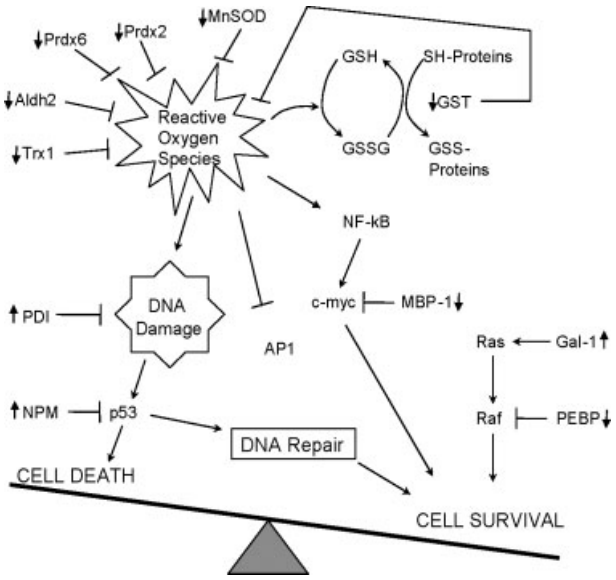

Figure 5. Cell death and survival are in a fine balance which is disrupted upon tumorigenesis. Small arrows in bold next to the protein indicate changes in level during tumor progression. Decreased levels of antioxidant enzymes such as MnSOD, Prdx2, Prdx6, Aldh2, and Trx1 were associated with accumulation of ROS, which in turn induce DNA damage and activation of NFkb. DNA damage in cells bearing normal p53, as Tm1 and Tm5, is often repaired. It is assumed that if the repair system is ineffective, then cells commit suicide (apoptosis). Tm1 and Tm5 accumulate large amounts of a repressor of p53 function (NPM). Decreased activity of p53 may favor the persistence of lesions in DNA, thus leading to mutations associated with neoplastic behavior. Accumulation of ROS and decreased expression of GST is associated with altered glutathionylation of proteins, a novel PTM that interferes with function of cytoplasmic and nuclear proteins in a yet undetermined manner. Accumulation of ROS may lead to activation of the protooncogene NF-kb, but inhibits the function of AP-1. NF-kB pathway involves myc. This pathway is likely activated in Tm1 and Tm5 cells, based on a decrease in the levels of MBP-1, which inhibits myc function, as it is involved in its degradation. Accumulation of increased levels of galectin-1 and decreased levels of PEBP may be associated with activation of RAS-RAF-MAP kinase pathway. Altogether, the proteomic findings support the view that there is an imbalance towards Tm1 and Tm5 cell survival, thus leading to cell growth and tumorigenesis.

These changes in the levels of these proteins in Tm1 and Tm5 can lead to a greater inhibition of p53-dependent apoptosis, a decrease in the inhibition of c-myc survival pathways and an increase in the signaling of Ras oncogene. These changes can explain why melanoma cells are not affected by

the increase of ROS [37], while other tumors are reported to undergo growth inhibition and activation of apoptotic pathways by increased levels of ROS [41].

Another objective of the current study was to extend the proteomic results to the identification of biological processes that could be affected by the observed differences in protein accumulation or depletion. We expected the extent of protein glutathionylation to be altered during melanoma progression, since GST is down-regulated in melanoma cells. The formation of disulfide bonds between oxidized glutathione (GSSG) and proteins is a normal defensive response of cells with higher levels of ROS [51]. Our data showed that glutathionylation levels in protein extracts obtained from Tm1 and Tm5 were, in fact, lower than in melan-a (Fig. 4). It has been demonstrated that glutathionylation can modify protein activity either negatively [52, 53] or positively [54]. Several proteins have been identified as targets of glutathionylation *in vivo* [55–57] and interestingly, of the 33 proteins identified in the present study as differentially accumulated during melan-a tumor progression, 18 (55%) are reported to be targets of glutathionylation. This suggests that glutathionylation, a posttranslational mechanism for the control of protein activity, may participate in melanoma tumor progression.

Both proteomic and SAGE data have identified the major molecules involved in the redox imbalance characteristic of melanomas. A likely consequence of this imbalance is the accumulation of mutations leading to melanoma heterogeneity and resistance to chemotherapeutic agents. Studies on the clinical significance of the expression pattern of these molecules are now underway.

Gustavo A. de Souza was a predoctoral fellow of Fundação de Amparo à Pesquisa do Estado de São Paulo – FAPESP (Process # 01/12971–3). This study was supported by FAPESP, FAPESP (CEPID), CNPq, and CNPq (Pronex).

5 References

[1] Castellano, M., Parmiani, G., *Melanoma Res.* 1999, *9*, 421–432.

[2] Walker, G. J., Flores, J. F., Glendensing, J. M., Lin, A. H. *et al.*, *Genes Chromosomes Cancer* 1998, *22*, 157–163.

[3] Soengas, M. S., Capodieci, P., Polsky, D., Mora, J. *et al.*, *Nature* 2001, *409*, 207–211.

[4] Iida, J., Pei, D., Kang, T., Simpson, M. A. *et al.*, *J. Biol. Chem.* 2001, *276*, 18786–18794.

[5] Nestle, F. O., *Oncogene* 2000, *19*, 6673–6679.

[6] Geertsen, R., Hofbauer, G., Kamarashev, J., Yue, F. Y., Dummer, R., *Int. J. Mol. Med.* 1999, *3*, 49–57.

[7] Hess, A. R., Seftor, E. A., Gardner, L. M., Carles-Kinch, K. *et al.*, *Cancer Res.* 2001, *61*, 3250–3255.

[8] Friedl, P., Brocker, E. B., Zanker, K. S., *Cell Adhes. Commun.* 1998, *6*, 225–236.

[9] Clark, W. H., Jr., Elder, D. E., Guerry, D, Braitman, L. E. *et al.*, *J. Natl. Cancer Inst.* 1989, *81*, 1893–1904.

[10] Berwick, M., Halpern, A., *Curr. Opin. Oncol.* 1997, *9*, 178–182.

[11] Meier, F., Satyamoorthy, K., Nesbit, M., Hsu, M. Y. *et al.*, *Front. Biosci.* 1998, *3*, D1005–D1010.

[12] Li, G., Herlyn, M., *Mol. Med. Today* 2000, *6*, 163–169.

[13] Clark, E. A., Golub, T. R., Lander, E. S., Hynes, R. O., *Nature* 2000, *406*, 532–535.

[14] Bittner, M., Meltzer, P., Chen, Y., Jiang, Y. *et al.*, *Nature* 2000, *406*, 536–540.

[15] Baldi, A., Battista, T., De Luca, A., Santini, D. *et al.*, *Exp. Dermatol.* 2003, *12*, 213–218.

[16] Rumpler, G., Becker, B., Hafner, C., McClelland, M. *et al.*, *Exp. Dermatol.* 2003, *12*, 761–771.

[17] Bernard, K., Litman, E., Fitzpatrick, J. L., Shellman, Y. G. *et al.*, *Cancer Res.* 2003, *63*, 6716–6725.

[18] Clauser, K. R., Hall, S. C., Smith, D. M., Webb, J. W. *et al.*, *Proc. Natl. Acad. Sci. USA* 1995, *92*, 5072–5076.

[19] Bennett, D. C., Cooper, P. J., Hart, I. R., *Int. J. Cancer* 1987, *39*, 414–418.

[20] Correa, M., Machado, M., Carneiro, C. R. W., Pesquero, J. B. *et al.*, *Int. J. Cancer* 2005, *114*, 356–363.

[21] Bradford, M. M., *Anal. Biochem.* 1976, *72*, 248–254.

[22] Rabilloud, T., Valette, C., Lawrence, J. J., *Electrophoresis* 1994, *15*, 1552–1558.

[23] Laemmli, U. K., *Nature* 1970, *227*, 680–685.

[24] Neuhoff, V., Arold, N., Taube, D., Ehrhardt, W., *Electrophoresis* 1998, *9*, 255–262.

[25] Williams, K. R., Stone, K. L., *Mol. Biotechnol.* 1997, *8*, 155–167.

[26] Silva, W. A., Jr., Covas, D. T., Panepucci, R. A., Proto-Siqueira, R. *et al.*, *Stem Cells* 2003, *21*, 661–669.

[27] Metarrese, P., Tinari, N., Semeraro, M. L., Natoli, C. *et al.*, *FEBS Lett.* 2000, *473*, 311–315.

[28] Gygi, S. P., Rochon, Y., Franza, B. R., Aebersold, R., *Mol. Cell Biol.* 1999, *19*, 1720–1730.

[29] Anderson, L., Seilhamer, J., *Electrophoresis* 1997, *18*, 533–537.

[30] Picardo, M., Grammatico, P., Roccella, F., Roccella, M. *et al.*, *J. Invest. Dermatol.* 1996, *107*, 322–326.

[31] Roblick, U. J., Hirschberg, D., Habermann, J. K., Palmberg, C. *et al.*, *Cell. Mol. Life Sci.* 2004, *61*, 1246–1255.

[32] Zhou, G., Li, H., DeCamp, D., Chen, S. *et al.*, *Mol. Cell. Proteomics* 2002, *1*, 117–124.

[33] Florenes, V. A., Faye, R. S., Maelandsmo, G. M., Nesland, J. M., Holm, R., *Clin. Cancer Res.* 2002, *6*, 3614–3620.

[34] Georgieva, J., Sinha, P., Schadendorf, D., *J. Clin. Pathol.* 2001, *54*, 229–235.

[35] Du, J., Widlund, H. R., Horstmann, M. A., Ramaswami, S. *et al.*, *Cancer Cell* 2004, *6*, 565–576.

[36] Mollenhauer, J., Deichmann, M., Helmke, B., Muller, H. *et al.*, *Int. J. Cancer* 2003, *105*, 149–157.

[37] Meyskens, F. L., Jr., McNulty, S. E., Buckmeier, J. A., Tohidian, N. B. *et al.*, *Free Radic. Biol. Med.* 2001, *31*, 799–808.

[38] de Gruijl, F. R., *Eur. J. Cancer* 1999, *35*, 2003–2009.

[39] Chedekel, M. R., *Photochem. Photobiol.* 1982, *35*, 881–885.

[40] Meyskens, F. L., Jr., Buckmeier, J. A., McNulty, S. E., Tohidian, N. B., *Clin. Cancer Res.* 1999, *5*, 1197–1202.

[41] Datta, K., Babbar, P., Srivastava, T., Sinha, S., Chattopadhyay, P., *Int. J. Biochem. Cell Biol.* 2002, *34*, 148–157.

[42] Armstrong, J. S., Steinauer, K. K., Hornung, B., Irish, J. M. *et al.*, *Cell Death Differ.* 2002, *9*, 252–263.

[43] Maiguel, D. A., Jones, L., Chakravarty, D., Yang, C., Carrier, F., *Mol. Cell. Biol.* 2004, *24*, 3703–3711.

[44] Subramanian, A., Miller, D. M., *J. Biol. Chem.* 2000, *275*, 5958–5965.

[45] Paz, A., Haklai, R., Elad-Sfadia, G., Ballan, E., Kloog, Y., *Oncogene* 2001, *20*, 7486–7493.

[46] Elad-Sfadia, G., Haklai, R., Ballan, E., Gabius, H. J., Kloog, Y., *J. Biol. Chem.* 2002, *277*, 37169–37175.

[47] Yeung, K., Seitz, T., Li, S., Janosch, P. *et al.*, *Nature* 1999, *401*, 173–177.

[48] Yeung, K., Janosch, P., McFerran, B., Rose, D. W. *et al., Mol. Cell Biol.* 2000, *20*, 3079–3085.

[49] Schuierer, M. M., Bataille, F., Hagan, S., Kolch, W., Bosserhoff, A. K., *Cancer Res.* 2004, *64*, 5186–5192.

[50] Tanaka, S., Uehara, T., Nomura, Y., *J. Biol. Chem.* 2000, *275*, 10388–10393.

[51] Cotgreave, I. A., Gerdes, R. G., *Biochem. Biophys. Res. Commun.* 1998, *242*, 1–9.

[52] Mohr, S., Hallak, H., de Boitte, A., Lapetina, E. G., Brune, B., *J. Biol. Chem.* 1999, *274*, 9427–9430.

[53] Casagrande, S., Bonetto, V., Fratelli, M., Gianazza, E. *et al.*, *Proc. Natl. Acad. Sci. USA* 2002, *99*, 9745–9749.

[54] Manevich, Y., Feinstein, S. I., Fisher, A. B., *Proc. Natl. Acad. Sci. USA* 2004, *101*, 3780–3785.

[55] Fratelli, M., Demol, H., Puype, M., Casagrande, S. *et al.*, *Proc. Natl. Acad. Sci. USA* 2002, *99*, 3505–3510.

[56] Fratelli, M., Demol, H., Puype, M., Casagrande, S. *et al.*, *Proteomics* 2003, *3*, 1154–1161.

[57] Lind, C., Gerdes, R., Hamnell, Y., Schuppe-Koistinen, I. *et al.*, *Arch. Biochem. Biophys.* 2002, *406*, 229–240.

